Journal of Biomolecular NMR (2005) 32: 31–40
DOI 10.1007/s10858-005-3340-5

Article

Bacterial expression and one-step purification of an isotope-labeled heterotrimeric G-protein α-subunit

Najmoutin G. Abdulaev[a,b], Cheng Zhang[c], Andy Dinh[c], Tony Ngo[a,b], Philip N. Bryan[a,b], Danielle M. Brabazon[d], John P. Marino[a,b,*] & Kevin D. Ridge[c]

[a]*Center for Advanced Research in Biotechnology, University of Maryland Biotechnology Institute, Rockville, MD 20850;* [b]*National Institute of Standards and Technology, Rockville, MD 20850;* [c]*Center for Membrane Biology, Department of Biochemistry and Molecular Biology, University of Texas Health Science Center, Houston, TX 77030;* [d]*Department of Chemistry, Loyola College in Maryland, Baltimore, MD 21210*

Received 17 December 2004; Accepted 8 February 2005

Key words: eukaryotic protein, G-protein, high-resolution, stable-isotope labeling, subtilisin, transducin

Abstract

Heterologous expression systems are often employed to generate sufficient quantities of isotope-labeled proteins for high-resolution NMR studies. Recently, the interaction between the prodomain region of subtilisin and an active, mutant form of the mature enzyme has been exploited to develop a cleavable affinity tag fusion system for one-step generation and purification of full-length soluble proteins obtained by inducible prokaryotic expression. As a first step towards applying high-resolution NMR methods to study heterotrimeric G-protein α-subunit (G_α) conformation and dynamics, the utility of this subtilisin prodomain fusion system for expressing and purifying an isotope-labeled G_α chimera (~40 kDa polypeptide) has been tested. The results show that a prodomain fused G_α chimera can be expressed to levels approaching 6–8 mg/l in minimal media and that the processed, mature protein exhibits properties similar to those of G_α isolated from natural sources. To assay for the functional integrity of the purified G_α chimera at NMR concentrations and probe for changes in the structure and dynamics of G_α that result from *activation*, ^{15}N-HSQC spectra of the GDP/Mg^{2+} bound form of G_α obtained in the absence and presence of aluminum fluoride, a well known activator of the GDP bound state, have been acquired. Comparisons of the ^{15}N-HSQC spectra reveals a number of changes in chemical shifts of the ^{1}HN, ^{15}N crosspeaks that are discussed with respect to expected changes in the protein conformation associated with G_α *activation*.

Introduction

Activation of a G-protein by an agonist-stimulated GPCR (R*) requires the propagation of structural signals from the receptor binding interface to the guanine nucleotide-binding pocket of the G-protein. Light-activated signaling of the retinal G-protein, transducin (G_t) by the GPCR rhodopsin serves as the paradigm for understanding the mechanisms governing R*/G-protein interactions [reviewed in (Ridge et al., 2003)]. In this signaling system, light activation of rhodopsin catalytically promotes the exchange of bound GDP for GTP in numerous G_t molecules to produce an active, GTP-bound form of the α-subunit ($G_{t\alpha}$). Activated $G_{t\alpha}$ triggers a cGMP phosphodiesterase mediated

*To whom correspondence should be addressed. E-mail: marino@carb.nist.gov

amplification cascade that ultimately culminates in hyperpolarization of the rod cell plasma membrane. $G_{t\alpha}$ has been the subject of numerous biochemical and biophysical investigations due to the natural abundance of G_t in the retina (Reichert and Hofmann, 1984; Guy et al., 1990; Cai et al., 2001; Ortiz and Bubis, 2001).

High-resolution crystal structures of isolated G_α subunits, including $G_{t\alpha}$ (Noel et al., 1993; Coleman et al., 1994; Lambright et al., 1994; Sondek et al., 1994; Mixon et al., 1995; Sunahara et al., 1997), as well as $G_{\alpha\beta\gamma}$ heterotrimeric complexes (Wall et al., 1995; Lambright et al., 1996), have provided important insights into the structural rearrangements accompanying guanine nucleotide exchange and the GTPase cycle. NMR methods have also been used to determine the solution structure of the GTPase activation domain of the α-subunit from the heterotrimeric G-protein G_s (Benjamin et al., 1995a, b). Similarly, crystallographic studies on inactive (dark-state) rhodopsin have provided valuable clues into the function of this light-sensing receptor and other related GPCRs (Palczewski et al., 2000; Teller et al., 2001; Okada et al., 2002, 2004; Li et al., 2004). However, high-resolution structural analysis of R*/G-protein complexes poses many unique challenges given the inherently dynamic nature of the interaction. While the crystallographic studies have been instrumental for obtaining static 'snapshot' structures of various states of G_α and the quiescent structure of rhodopsin, and biochemical/biophysical approaches have provided a wealth of information about the nature of R^*/G_t interactions, a detailed structural framework of the R^*/G_t complex(es) remains poorly defined. Clearly, a comprehensive description of the structures involved in these dynamic interactions would provide important insights into the mechanisms governing activated GPCR/G-protein interactions.

Although some progress has been made in recent years toward the successful expression of properly folded soluble eukaryotic proteins in prokaryotic hosts, in most cases these proteins tend to be limited to less than 30 kDa and lack the common post-translational modifications found on many eukaryotic proteins (Baneyx, 1999). Several major advantages of prokaryotic cell expression over eukaryotic cell expression include the wide availability of tightly regulated inducible systems, relatively short time periods for target protein expression, and controlled growth in minimal media liquid suspensions supplemented with various isotope labeled nitrogen and carbon compounds. As such, even cells that produce only limited amounts of a given protein can be grown to densities that allow for the isolation of sufficient amounts of isotope labeled protein for high-resolution NMR studies. With regard to purification, the use of affinity tags for the isolation of heterologously expressed eukaryotic proteins has now become commonplace. Numerous investigators have employed the hexahistidine (His_6) tag in combination with immobilized metal affinity chromatography (IMAC) to facilitate the purification of expressed proteins (Porath et al., 1975; Schmitt et al., 1993). As the His_6 tag can often interfere with the structure and/or function of the expressed protein, particularly in those cases where the amino- and/or carboxyl-terminus may represent a functionally interacting site(s), as is thought to be the case for G_α (Hamm et al., 1988; Hamm, 2001), a cleavage site for a sequence specific protease (e.g., TEV protease, thrombin, Factor X, enterokinase, etc.) is typically introduced between the protein of interest and the His_6 sequence. However, subsequent removal of the His_6 tag from milligram quantities of protein after IMAC purification can be relatively costly, necessitates the need for additional purification steps to remove the protease, and typically results in additional amino acids remaining on the protein of interest, which may also adversely influence structure and/or function.

Previous attempts to generate milligram quantities of functional $G_{t\alpha}$ through recombinant prokaryotic (bacterial) overexpression have routinely failed due to insolubility of the expressed protein (Skiba et al., 1996). However, chimeric G-protein α-subunits comprised of various sequences from $G_{t\alpha}$ and $G_{i1\alpha}$ that are more amenable to soluble overproduction in bacterial hosts have been designed (Skiba et al., 1996; Natochin et al., 1999). One such chimera, termed Chi6, contains amino acids 1–215 and 295–350 from $G_{t\alpha}$ with an intervening sequence (amino acids 216–294) from $G_{i1\alpha}$. A gene that encodes an amino-terminal His_6-tagged version of Chi6 has been successfully expressed in a soluble form in *E. coli* and the protein isolated by IMAC

(Skiba et al., 1996). Biochemical and biophysical characterization of Chi6 has shown that it exhibits '$G_{t\alpha}$-like' properties in a variety of assays (Skiba et al., 1996). Further, Chi6 has been crystallized as part of a reconstituted $G_{\alpha\beta\gamma}$ heterotrimer (Lambright et al., 1996) and in complex with the RGS domain of RGS9-1 and a fragment of the γ-subunit of cGMP phosphodiesterase (Slep et al., 2001). Using the His_6-tagged version of Chi6, we have been able to purify ~3 mg of soluble protein from one liter of bacterial culture grown in rich media [e.g., Luria–Bertani (LB) media]. However, efforts to obtain comparable amounts of soluble, isotope-labeled samples from bacterial cultures grown in minimal media formulations, which often result in reduced protein yields, have not been successful. In addition, the Chi6 reconstituted heterotrimer has reproducibly shown a 25–30% lower level of rhodopsin stimulated GDP–GTP exchange activity in our hands when compared to $G_{t\alpha\beta\gamma}$ and reconstituted $G_{t\alpha}$ + $G_{t\beta\gamma}$ isolated from bovine retina, both of which show similar kinetics and levels of guanine nucleotide exchange activity (N.G.A. and K.D.R., unpublished results). This lower level of R* stimulated GDP–GTP exchange observed for the Chi6 reconstituted heterotrimer may be due to the presence of the amino-terminal His_6 tag on Chi6, as the amino-terminus of G-protein α-subunits is considered a major R* interaction site (Hamm et al., 1988; Hamm, 2001). Further, purified His_6-tagged Chi6 has been found to undergo a relatively rapid time-dependent aggregation when concentrated to levels necessary for NMR studies.

Given the limitation of previously described protocols for heterologous expression and His_6-tagged IMAC affinity purification schemes, strategies to overexpress soluble, isotope-labeled full-length Chi6 devoid of the His_6 tag have been pursued. Here we describe a coupled expression/purification approach, based on the interaction between the prodomain region of subtilisin BPN' and an active, mutant form of subtilisin BPN' (Ruan et al., 2004), that allows for expression and one-step isolation of milligram amounts of an isotope-labeled, full-length G_α chimera. Isotope-labeled G_α chimera is further shown to be amenable to high-resolution structural analysis by NMR.

Materials and methods[1]

Materials

Restriction endonucleases and DNA modifying enzymes were from New England Biolabs (Beverly, MA) and Complete™ EDTA free protease inhibitor tablets were from Roche Applied Science (Indianapolis, IN). The QuikChange II site directed mutagenesis kit was from Stratagene (La Jolla, CA), and Blue-Sepharose CL-6B was from Amersham Biosciences (Piscataway, NJ). Phenylmethylsulfonyl fluoride (PMSF), isopropyl-β-D-thiogalactopyranoside (IPTG), GDP, and ^2H_2O were from Sigma (St. Louis, MO), $^{15}NH_4Cl$ and d_{11}Tris were from Spectra Stable Isotopes (Columbia, MD), and bovine retinae were from W. Lawson Co. (Lincoln, NE). A plasmid containing the gene for Chi6, an amino-terminal His_6-tagged G_α chimera that contains amino acids 1–215 and 295–350 from $G_{t\alpha}$ with an intervening sequence (amino acids 216–294) from $G_{i1\alpha}$ (Skiba et al., 1996), was provided by Dr. N. Skiba. The pG58 expression vector, a prodomain fusion vector encoding the modified 77 amino acid prodomain region of subtilisin BPN', and the S189 subtilisin BPN' mutant have been described (Ruan et al., 2004).

Insertion of the chimeric G_α gene into pG58

A Chi6 gene lacking the amino-terminal His_6-tag and linker region was first generated using the QuikChange II mutagenesis kit according to the manufacturer's instructions. The complementary oligonucleotide primers were synthesized on an ABI 340A DNA synthesizer and the resulting gene sequence confirmed by DNA sequencing. The resulting gene was excised from the plasmid by linearizing with *Nco*I, filling in the *Nco*I overhang with the Klenow fragment of DNA polymerase I, and then digesting with *Hin*dIII. For insertion of this fragment into pG58, the T7 promoter based prodomain fusion expression vector (Ruan et al., 2004), this plasmid was first linearized with *Eco*RI,

[1]Certain commercial equipment, instruments, and materials are identified in this paper in order to specify the experimental procedure. Such identification does not imply recommendation or endorsement by the National Institute of Standards and Technology, nor does it imply that the material or equipment identified is necessarily the best available for the purpose.

the overhang filled in with the Klenow enzyme, and then digested with *Hin*dIII. Ligation of the excised Chi6 gene with pG58 recreates the *Eco*RI site as an 'in frame' fusion between a mutant version of the 77 amino acid subtilisin BPN' prodomain and the target gene sequence. The mutant prodomain (proR8FKAM) has been altered such that amino acids 16–21 (QTMSTM) are replaced with SGIK, amino acids 74–77 (AKAY) are replaced with FKAM and A23C, K27Q, V37L, Q40C, H72K and H75K point mutations are included (Ruan et al., 2004). The *Eco*RI site was subsequently removed by using QuikChange II yielding fusion genes encoding the prodomain sequence terminated by the FKAM sequence followed by the initiator Met of the Chi6 protein. Cleavage of the prodomain by S189 subtilisin BPN' occurs between the Met of the FKAM sequence and Met-1 of the target protein (Ruan et al., 2004), yielding full-length protein devoid of any prodomain residues.

Expression of the prodomain/G_α fusion protein in E. coli

E. coli BL21 (DE3) cells harboring the pG58 expression vector containing the prodomain/Chi6 fusion were grown in 500 ml of LB media or minimal media in the presence of 100 μg/ml ampicillin at 26 °C to A_{550} ~0.3, and then induced with 30 μM IPTG for 12 h at 26 °C. For isotopic labeling of G_α, the transformed cells were grown in minimal media supplemented with 1 g/l of $^{15}NH_4Cl$ as the sole nitrogen source. The cell pellet was resuspended in 50 mM Tris–HCl, pH 8.0, containing 50 mM NaCl, 5 mM $MgCl_2$, 150 μM GDP, 5 mM β-mercaptoethanol, 0.1 mM PMSF, and a protease inhibitor tablet (Buffer A) and then disrupted by sonication. The supernatant obtained by centrifugation of the cell lysate at 100,000 × *g* for 45 min was collected and processed immediately or stored at −80 °C.

Purification of G_α from the prodomain released fusion protein

The clarified supernatant containing the prodomain/Chi6 fusion was loaded onto a S189 subtilisin BPN' HiTrap NHS column prepared as described (Ruan et al., 2004). The column was washed with 20 volumes of Buffer A to remove contaminating proteins. The total time for the binding and washing steps ranged from 30 to 40 min, a period during which cleavage of the fusion by S189 subtilisin BPN' is negligible. The prodomain released G_α subunit, which we call ChiT, was eluted in 10 mM Tris–HCl, pH 7.5, containing 100 mM NaCl, 5 mM $MgCl_2$, 50 μM GDP, 2.5 mM DTT, and 0.1 mM PMSF (Buffer B) after maintaining the column for 10–12 h at room temperature. For NMR analysis, the purified, isotope-labeled protein was concentrated and dialyzed against NMR Buffer (25 mM d_{11}Tris–HCl, pH 7.5, containing 100 mM NaCl, 5 mM magnesium acetate, 2.5 mM DTT, 50 μM GDP and 5% glycerol), or eluted directly from the column in this same buffer. All G_α constructs were purified in a similar manner.

Construction of G_α mutants

The W127F, W207F and W254F mutants were generated using QuikChange II according to the manufacturer's instructions using the pG58 expression vector encoding the prodomain/Chi6 fusion as a template. The complementary oligonucleotide primers were synthesized on an ABI 340A DNA synthesizer and the resulting mutations verified by DNA sequencing.

Isolation of $G_{t\alpha}$ from the G_t heterotrimer

G_t was prepared from bovine retina by the method of Fung et al. (Fung et al., 1981). To separate the $G_{t\alpha}$ and $G_{t\beta\gamma}$ subunits, purified G_t in Buffer B containing 50% glycerol was diluted three times with the same buffer without glycerol and applied to Blue-Sepharose CL-6B equilibrated with 10 mM MOPS, pH 7.5, containing 5 mM magnesium acetate, and 2.5 mM DTT. $G_{t\beta\gamma}$ does not bind to the resin and is obtained from the flow through. The column was washed with equilibration buffer and $G_{t\alpha}$ eluted in the same buffer containing 2 M NaCl. The purified $G_{t\alpha}$ subunit was concentrated by dialysis in Buffer B containing 50% glycerol and stored at −20 °C.

NMR spectroscopy of isotope labeled G_α

^{15}N-HSQC water flip-back, water gate experiments (Grzesiek and Bax, 1993) were recorded at 30 °C on a Bruker AVANCE 600 MHz

spectrometer (Bruker Instruments, Billerica, MA) equipped with a triple-resonance ^{1}H, ^{13}C, ^{15}N Z-axis gradient cryoprobe and linear amplifiers on all three channels. Spectra were collected on ^{15}N-labeled ChiT samples in NMR Buffer using sweep widths of 7200 Hz in ω_2 and 2000 Hz in ω_1, 2 K by 128 complex data points in t_2 and t_1, respectively, (t_{1max} = 293 ms and t_{2max} = 64 ms) and 128 scans per increment. All spectra were processed and analyzed on a SGI UNIX workstation using NMRPipe (Delaglio et al., 1995). The AlF_4^- adduct of the GDP/Mg^{2+} bound G_α was formed by addition of NaF (10 mM) and $AlCl_3$(300 μM) directly to the NMR tube.

Other methods

Mass spectrometric analysis of the purified, expressed G_α chimera was performed essentially as described (Abdulaev et al., 2000). Protein samples were analyzed by SDS-PAGE (Laemmli, 1970) with a 5% stacking gel and a 12% resolving gel and visualized by Coomassie Blue staining. Protein determinations were done using the method of Peterson (Peterson, 1977) with BSA as the standard.

Results and discussion

Expression and purification of a chimeric G_α subunit via a subtilisin BPN' prodomain fusion

Numerous studies have utilized heterologous expression as a means to examine the structure and function of soluble eukaryotic proteins. By far, the most prevalent hosts for the expression of eukaryotic proteins are yeast, insect, and mammalian cells. However, focused efforts aimed at maximizing the inducible expression of properly folded and uniformly processed eukaryotic proteins in prokaryotic cells would clearly provide advantages for generating isotope-labeled proteins for high-resolution NMR studies. To this end, the use of a subtilisin BPN' prodomain fusion for the expression and purification of a chimeric G_α subunit was pursued. The serine protease subtilisin (EC 3.4.21.14) is among the most thoroughly studied enzymes. Like many proteases, subtilisin is expressed as a zymogen precursor containing a 30 amino acid presequence, which functions as a signal peptide for protein secretion and is ultimately cleaved by a signal peptidase, and a 77 amino acid prodomain that is positioned between the signal sequence and the 275 amino acid mature enzyme. Several studies have shown that the prodomain region actively participates in the folding of subtilisin [reviewed in (Bryan, 2002)]. Once folded, the prodomain is removed from subtilisin by an autocatalytic process. However, the cleaved prodomain can still bind tightly (nM affinity) to the active enzyme, although it is typically degraded by free subtilisin. By optimizing the binding and catalytic activities of subtilisin BPN', as well as its recognition of the prodomain region through systematic protein engineering, Bryan and colleagues (Ruan et al., 2004) have successfully developed an expression/purification approach that has facilitated the high-level expression and one-step purification of *Aequoria Victoria* green fluorescent protein (GFP) and other soluble proteins of interest. Our rationale for testing the subtilisin BPN' prodomain fusion system as a method for expressing/purifying Chi6 in minimal media was twofold. First, expression of the His_6-tagged version of Chi6 in minimal media formulations compatible with isotope labeling resulted in significantly reduced cellular expression levels when compared with those cells grown in rich media. Further, virtually all of the expressed His_6-tagged Chi6 protein was found in inclusion bodies. Our hypothesis was that fusion with the prodomain region of subtilisin BPN' might enhance overall G_α solubility, resulting in a greater recovery of protein from the soluble cell lysate. Second, such an approach would alleviate the need for the amino-terminal His_6 tag, which appears to interfere with R* interactions when part of the reconstituted heterotrimer.

For our work, the gene for Chi6 devoid of the amino-terminal His_6 tag sequence was placed downstream from the 77 amino acid prodomain of subtilisin BPN' in the pG58 expression vector and transformed into BL21 cells. After growth in minimal media supplemented with $^{15}NH_4Cl$, as the sole nitrogen source, and IPTG induction at ambient temperature, the soluble extract was applied to the immobilized S189 mutant of subtilisin BPN'. Our expression results using the proR8FKAM fusion (Figure 1a) clearly show that the fusion protein is only present after IPTG induction (Figure 1a, lane 2) and that a majority

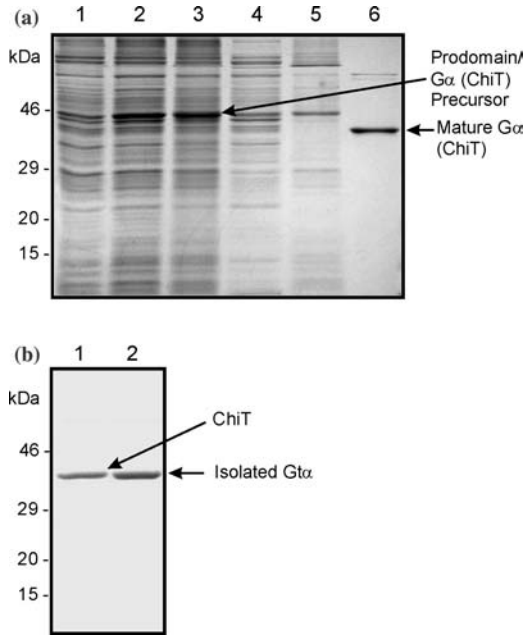

Figure 1. Expression and purification of ChiT. SDS-PAGE analysis of (a) *E. coli* expressed and purified ChiT, a G_α chimera, using the proR8FKAM fusion and immobilized S189 subtilisin BPN' approach (Ruan et al., 2004), and (b) purified ChiT and native $G_{t\alpha}$ purified from bovine retina. (a) Lanes are as follows: (1) total cell extract from uninduced cells; (2) total cell extract from IPTG induced cells; (3) soluble extract from IPTG induced cells; (4) insoluble fraction from IPTG induced cells; (5) low pH elution of proteins retained on immobilized subtilisin after brief washing; (6) eluted mature protein obtained after extensive washing to remove contaminating proteins. Note positions of the precursor fusion and the processed mature forms. (b) Lane 1, purified ChiT; lane 2, purified $G_{t\alpha}$. Protein bands were visualized using Coomassie blue. The positions of molecular mass standards are shown on the left.

of the protein, but not all, is present in the supernatant of the cell lysate (Figure 1a, lane 3). Further, the soluble fraction containing the fusion protein binds to the immobilized enzyme (Figure 1a, lane 5) and after extensive washing to remove contaminating proteins, the mature, full length protein, which we call ChiT, is subsequently cleaved from the prodomain by the immobilized protease during an overnight incubation at ambient temperature and then eluted from the column in a highly purified form (Figure 1a, lane 6). On occasion, some minor higher molecular mass proteins were also apparent in the eluted ChiT samples. The highest molecular mass protein observed appears to represent an SDS induced ChiT aggregate, as it cross reacts with an anti-$G_{t\alpha}$ antibody upon immunoblot analysis, and is variably observed. The faint yet distinct band just below this ChiT aggregate may correspond to a minor protein contaminant, which is also sporadically observed between the various preparations (note the absence of both higher molecular mass proteins in Figure 1b, lane 1). Based on the results of numerous experiments, however, we estimate that our preparations of mature ChiT are typically >95% pure, and the very low concentration of any possible contaminant in some of the samples has so far not interfered with any of the NMR measurements. It should also be noted that the activity of S189 subtilisin BPN' toward proR8FKAM fusion proteins is sensitive to fluoride and chloride concentrations, and as such, increasing concentrations of these anions can accelerate the cleavage reaction (Ruan et al., 2004). For our studies, however, we did not specifically incorporate this 'chemical trigger' step, but rather relied on the fact that under our purification conditions, which included 100 mM NaCl in the elution buffer, functional prodomain released full-length G_α (ChiT) could be obtained.

Using the subtilisin BPN' prodomain fusion system, we now routinely purify 6–8 mg of soluble, isotope-labeled ChiT from a one liter shake flask culture in a single column run. We attribute this high yield of mature ChiT relative to His_6-tagged Chi6 to be a consequence of enhanced soluble expression conferred by the proR8FKAM fusion as comparisons between the amount of protein in the soluble extracts vs. the insoluble fractions clearly show that the precursor form of ChiT is largely expressed in a soluble form, whereas His_6-tagged Chi6 is predominantly found in an insoluble form. Analysis of purified ChiT also showed that it co-migrates with $G_{t\alpha}$ isolated from bovine retina (Figure 1b), and that the apparent molecular mass obtained by SDS-PAGE (~40 kDa) is in agreement with results from mass spectrometry that show an average molecular mass of 40,150 Da ($n = 11$). Further, unlike His_6-tagged Chi6 reconstituted heterotrimer, ChiT reconstituted heterotrimer shows nearly the same kinetics and levels of R* stimulated guanine nucleotide exchange activity as $G_{t\alpha\beta\gamma}$ and reconstituted $G_{t\alpha} + G_{t\beta\gamma}$ isolated from bovine retina (N.G.A. and K.D.R., unpublished results).

NMR analysis of the ^{15}N-labeled GDP/Mg^{2+} bound form of ChiT

As an initial assay of the spectroscopic properties of ChiT and to judge its suitability for NMR analysis, we have collected an ^{15}N-HSQC on a uniformly ^{15}N-labeled sample of ChiT (~150 μM) in complex with GDP/Mg^{2+} in NMR buffer at 30 °C using a TXI HCN NMR cryoprobe operating at 600 MHz. Overall, the ^{15}N-HSQC spectrum of ChiT (Figure 2a) is relatively well dispersed and roughly 340 ^{1}HN, ^{15}N crosspeaks can be readily identified (backbone and side chain) which may be compared with the 345 non-proline backbone and 52 Asn and Gln sidechain ^{1}HN, ^{15}N crosspeaks expected based on the amino acid sequence of ChiT. The observed ^{1}HN, ^{15}N crosspeaks also exhibit line widths that are relatively uniform and as would be expected for an α/β protein of this size. In addition, while ChiT is found to slowly aggregate at higher concentrations (>500 μM), ChiT samples in NMR buffer conditions described here have been found to remain soluble and stable over multiple days at 30 °C at a concentrations up to ~250 μM, which allows for the practical application of multi-dimensional triple-resonance experiments to ^{2}H, ^{13}C, ^{15}N-labeled ChiT samples using a cryoprobe. While conventional ^{15}N-HSQC correlation has been used in this study to evaluate ^{15}N-labeled ChiT, given its molecular weight, application of ^{15}N-TROSY (Pervushin et al., 1997) correlation should provide improved spectral resolution and sensitivity. Initial application of ^{15}N-TROSY to ^{15}N-labeled ChiT at magnetic field strengths of 600 and 800 MHz (D.M.B. and J.P.M., unpublished results), however, has not realized the anticipated spectral enhancement. While ChiT backbone dynamics may be a factor in the performance of the TROSY, application of TROSY to ^{2}H,^{15}N-labeled ChiT samples will likely be required to achieve significant gains in sensitivity and resolution using this method.

Assignment of Trp indole ^{1}HN and ^{15}N resonances using ChiT mutants

$G_{t\alpha}$ contains two Trp residues at positions 127 and 207, while ChiT contains an additional Trp residue at position 254 that is derived from the $G_{i1\alpha}$ sequence. It is known from mutagenesis (Faurobert et al., 1993) and crystallographic studies (Noel et al., 1993) of $G_{t\alpha}$ that the environment of Trp-207 changes upon activation. This residue, which is located in the switch II region of $G_{t\alpha}$, also undergoes fluorescence changes accompanying GDP/GTP exchange during R*/heterotrimer interactions. Similar fluorescence changes can be observed in the GDP-bound form of Gt_{α} in the

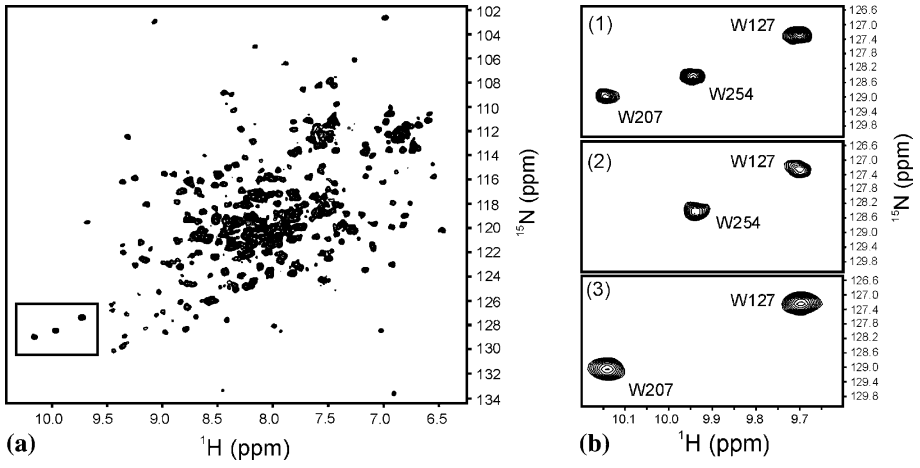

Figure 2. (a) ^{15}N-HSQC of GDP/Mg^{2+} bound wild-type ChiT acquired in NMR buffer at 30 °C. The spectra were collected as described in Material and methods. The assigned ^{1}HN,^{15}N crosspeaks for the three Trp indoles are boxed. Note that while $G_{t\alpha}$ contains only two Trp residues (at positions 127 and 207), ChiT contains an additional Trp at position 254 from the $G_{i1\alpha}$ sequence. (b) Expansion of the region of the ^{15}N-HSQC spectra containing the ^{1}HN,^{15}N crosspeaks for the tryptophan indoles as observed for the GDP/Mg^{2+} bound wild-type ChiT (1), the mutant W207F (2) and the mutant W254F (3). Assignments are indicated on the ^{1}HN,^{15}N crosspeaks in each spectra.

presence of aluminum fluoride (Phillips and Cerione, 1988; Antonny and Chabre, 1992). Given these observations, we anticipated that the indole resonances of ChiT could provide useful initial probes of structural changes in G_α that resulted from *activation* either through aluminum fluoride adduct formation or guanine nucleotide exchange. These resonances were therefore assigned through individual mutation of the three Trp residues to generate constructs W127F, W207F and W254F. By comparison of wild-type and mutant ^{15}N-HSQC spectra, assignment has been made via an absence of the indole ^{1}HN, ^{15}N crosspeak belonging to the mutated residue (Figure 2b). With the exception of mutant W127F, which yielded a uniformly exchange broadened HSQC spectra, assignment could be made directly using these ChiT mutants since the mutations did not significantly perturb the protein structure and therefore did not alter the pattern of chemical shifts observed in the HSQC spectra relative to the wild-type protein. Since the HSQC spectrum of W127F could not be used to make a direct assignment, the third crosspeak observed in the downfield region of the HSQC where indole ^{1}HN, ^{15}N correlations are expected has been tentatively assigned to W127 based on chemical shifts and a process of elimination.

NMR analysis of the ^{15}N isotope-labeled GDP-AlF_4^-/Mg^{2+} bound form of ChiT

Aluminum fluoride is a well known activator of monomeric and heterotrimeric G-proteins. In the

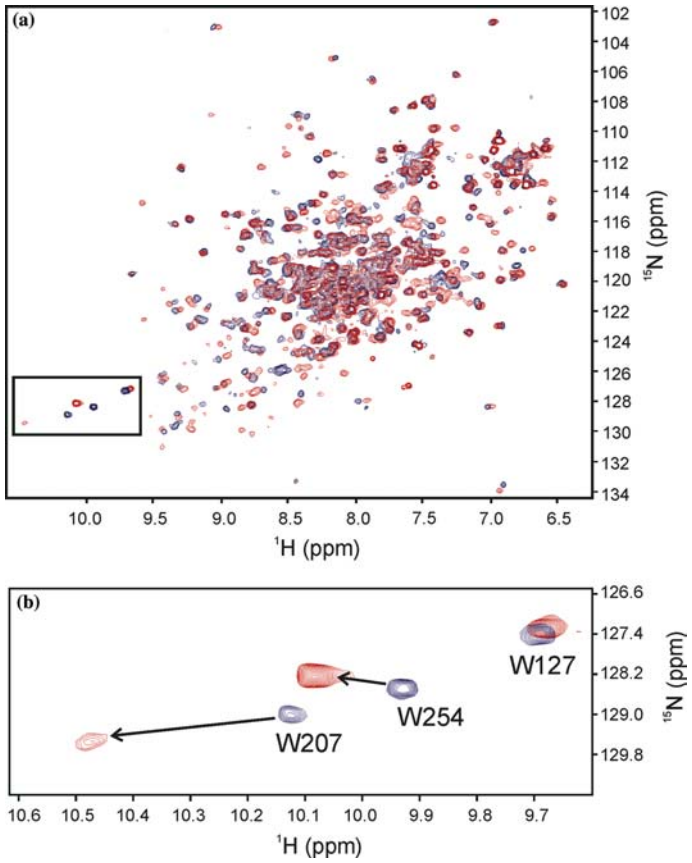

Figure 3. Overlay of ^{15}N-HSQC spectra of GDP/Mg^{2+} (blue) and GDP-AlF_4^-/Mg^{2+} (red) bound ChiT in NMR buffer at 30 °C using parameters described in Materials and methods. Differences in the conformations are manifested in a number of changes in chemical shifts of the ^{1}HN, ^{15}N crosspeaks. The region of the 2D spectrum containing the three Trp indole crosspeaks is boxed. (b) Expansion of the Trp indole resonance region of the ^{15}N-HSQC spectra of GDP/Mg^{2+} (blue) and GDP-AlF_4^-/Mg^{2+} (red) bound ChiT. Changes in the chemical shifts for the assigned ^{1}HN, ^{15}N crosspeaks for two of the three Trp indoles are indicated by arrows.

presence of GDP and Mg^{2+}, AlF_4^- mimics the γ-phosphate of G_αGTP and promotes changes in protein conformation (Phillips and Cerione, 1988; Higashijima et al., 1991; Antonny and Chabre, 1992). Thus, G_αGDP-AlF_4^-/Mg^{2+} is considered a representation of the activated conformation (Noel et al., 1993; Sunahara et al., 1997). Since the AlF_4^- -dependent conformational change tests whether GDP is present in the guanine nucleotide binding pocket of G_α, as well as determines the ability of the protein to undergo *activating* conformational changes, the GDP/Mg^{2+} bound form of ChiT (Figure 3) was titrated with NaF (10 mM) and $AlCl_3$(300 μM) to form the AlF_4^-adduct. An overlay of the ^{15}N-HSQC's for the GDP/Mg^{2+} and the GDP-AlF_4^-/Mg^{2+} bound forms of ^{15}N-labeled ChiT (Figure 3) shows that a number of amide resonances shift as a result of AlF_4^- adduct formation and suggest changes in the protein conformation. For example, two of the three Trp indole ^{1}HN, ^{15}N correlations (Figure 3b) display distinct chemical shift changes as a result of the formation of the *activated* state. The observed perturbations in the indole ^{1}HN and ^{15}N chemical shifts of Trp-207 and Trp-254 are consistent with observed differences in the crystal structures of the *ground* and AlF_4^- *activated* states of G_α (Sondek et al., 1994) and previous measurements that show a change in tryptophan fluorescence associated with W207 upon AlF_4^- adduct formation (Phillips and Cerione, 1988; Antonny and Chabre, 1992). In particular, changes in the chemical shifts of the indole ^{1}HN and ^{15}N resonances of residue W207 are consistent with a change in the conformation of the switch II region upon *activation* which results, in among other structural changes, a rotation of the Trp-207 side chain from a solvent exposed conformation into an ordered interaction with residues from the α_3 helix (Figure 4). A change in the chemical shifts of the indole ^{1}HN and ^{15}N resonances of residue W254 is also expected based on the crystal structures since this residue is found in the loop connecting α_3 and β_5 and residues within switch II pack against W254 in the activated state (Figure 4). In contrast, the observation of no significant change in chemical shifts of the indole ^{1}HN and ^{15}N resonances of residue W127 is consistent with previous observations in the crystal structures (Lambright et al., 1994; Sondek et al., 1994) that the helical domain

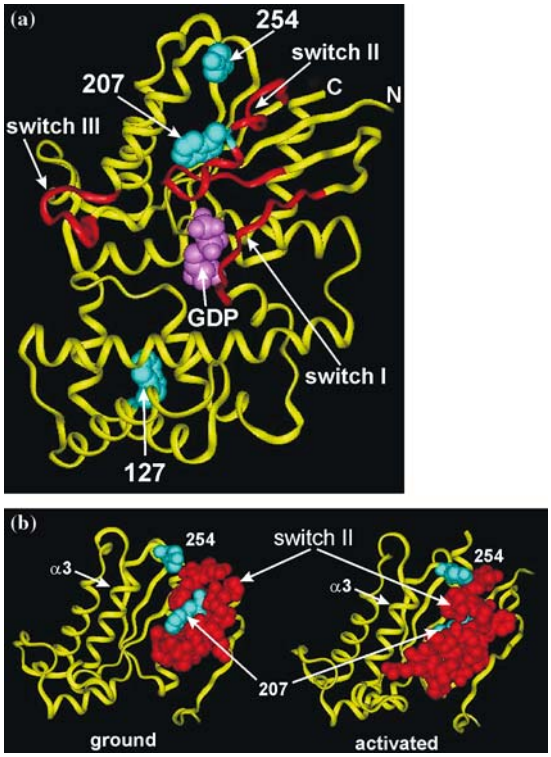

Figure 4. (a) A ribbon representation of the GDP/Mg^{2+} bound form of G_α (PDB code 1TAG) as observed in the crystal structures at 1.8 Å showing the relative positions of the Trp residues, as well as bound GDP and previously defined conformational switch I, II and III regions associated with α-subunit *activation*. The backbone trace of the switch regions I, II and III are shown in red and the remaining backbone trace is shown in yellow. The amino- and carboxyl-termini are labeled with N and C, respectively. Trp residues 127, 207, and 254 are in light blue and shown in CPK. (b) Conformational differences in switch II between the GDP/Mg^{2+} bound (left, PDB code 1TAG) and activated GDP-AlF_4^-/Mg^{2+} bound (right, PDB code 1TAD) forms of G_α as observed in the crystal structures at 1.8 Å and 1.7 Å, respectively (Sondek et al., 1994). The backbones are shown in yellow ribbon, with the switch II region in red and shown in CPK to highlight the conformational changes this region undergoes as a result of *activation*. Trp residues 207 and 254 are in light blue and shown in CPK.

of G_α, within which this residue is found, does not exhibit any significant structural changes between the *ground* and AlF_4^- *activated* states.

Conclusion

We have demonstrated an ability to obtain milligram quantities of a full-length, isotope-labeled heterotrimeric G-protein α-subunit chimera (ChiT) that is amenable to functional study under

NMR experimental conditions. A key aspect of this work has been the application of a new expression and purification approach (Ruan et al., 2004) that is based on the interaction between the prodomain region of subtilisin BPN' and an active, mutant form of subtilisin BPN', that allows for the one-step generation and purification of full-length G_α obtained by inducible prokaryotic expression. Preliminary NMR analysis of ChiT demonstrates that backbone and selected side chain resonances can be used to map at atomic resolution changes in the structure and dynamics of G_α. Using high-resolution NMR methods, we are now investigating the solution structures of G_α in various states and anticipate that such methods will provide new insights into G_α function.

Acknowledgement

We thank Fenhong Song (UMBI) for oligonucleotide synthesis, Jaya Jagadeesh (UMBI) for technical assistance in the early stages of this work, and Kris Palczewski (University of Washington) for helpful comments on the manuscript. This work was supported by a Karl Kirschgessner Foundation award to K.D.R., NIH Grant GM42560 to P.N.B., and Research Corporation Grant CC5250 to D.M.B. NMR instrumentation was supported in part by the W. M. Keck Foundation.

References

Abdulaev, N.G. Ngo, T. Chen, R.W. Lu, Z. and Ridge, K.D. (2000) *J. Biol. Chem.*, **275** (50) 39354–39363.

Antonny, B. and Chabre, M. (1992) *J. Biol. Chem.*, **267** (10) 6710–6718.

Baneyx, F. (1999) *Curr. Opin. Biotech.*, **10** (5) 411–421.

Benjamin, D.R. Markby, D.W. Bourne, H.R. and Kuntz, I.D. (1995a) *J. Mol. Biol.*, **254** (4) 681–691.

Benjamin, D.R. Markby, D.W. Bourne, H.R. and Kuntz, I.D. (1995b) *Biochemistry*, **34** (1) 155–162.

Bryan, P.N. (2002) *Chem. Rev.*, **102** (12) 4805–4815.

Cai, K. Itoh, Y. and Khorana, F.C. (2001) *Proc. Natl. Acad. Sci. USA*, **98** (9) 4877–4882.

Coleman, D.E. Berghuis, A.M. Lee, E. Linder, M.E. Gilman, A.G. and Sprang, S.R. (1994) *Science*, **265** (5177) 1405–1412.

Delaglio, F. Grzesiek, S. Vuister, G.W. Zhu, G. Pfeifer, J. and Bax, A. (1995) *J. Biomol. NMR*, **6** (3) 277–293.

Faurobert, E. Ottobruc, A. Chardin, P. and Chabre, M. (1993) *EMBO J.*, **12** (11) 4191–4198.

Fung, B.K.K. Hurley, J.B. and Stryer, L. (1981) *Proc. Natl. Acad. Sci. USA*, **78** (1) 152–156.

Grzesiek, S. and Bax, A. (1993) *J. Am. Chem. Soc.*, **115** (26) 12593–12594.

Guy, P.M. Koland, J.G. and Cerione, R.A. (1990) *Biochemistry*, **29** (30) 6954–6964.

Hamm, H.E. (2001) *Proc. Natl. Acad. Sci. USA*, **98** (9) 4819–4821.

Hamm, H.E. Deretic, D. Arendt, A. Hargrave, P.A. Koenig, B. and Hofmann, K.P. (1988) *Science*, **241** (4867) 832 835.

Higashijima, T. Graziano, M.P. Suga, H. Kainosho, M. and Gilman, A. (1991) *J. Biol. Chem.*, **266** (6) 3396–3401.

Laemmli, U.K. (1970) *Nature*, **277** (5259) 680–685.

Lambright, D.G. Noel, J.P. Hamm, H.E. and Sigler, P.B. (1994) *Nature*, **369** (6482) 621–628.

Lambright, D.G. Sondek, J. Bohm, A. Skiba, N.P. Hamm, H.E. and Sigler, P.B. (1996) *Nature*, **379** (6563) 311–319.

Li, J. Edwards, P.C. Burghammer, M. Villa, C. and Schertler, G.F. (2004) *J. Mol. Biol.*, **343** (5) 1409–1438.

Mixon, M.B. Lee, E. Coleman, D.E. Berghuis, A.M. Gilman, A.G. and Sprang, S.R. (1995) *Science*, **270** (5238) 954–960.

Natochin, M. Granovsky, A.E. Muradov, K.G. and Artemyev, N.O. (1999) *J. Biol. Chem.*, **274** (12) 7865–7869.

Noel, J.P. Hamm, H.E. and Sigler, P.B. (1993) *Nature*, **366** (6456) 654–663.

Okada, T. Fujiyoshi, Y. Silow, M. Navarro, J. Landau, E.M. and Shichida, Y. (2002) *Proc. Natl. Acad. Sci. USA*, **99** (9) 5982–5987.

Okada, T. Sugihara, M. Bondar, A.N. Elstner, M. Entel, P. and Buss, V. (2004) *J. Mol. Biol.*, **342** (2) 571–583.

Ortiz, J.O. and Bubis, J. (2001) *Arch. Biochem. Biophys.*, **387** (2) 233–242.

Palczewski, K. Kumasaka, T. Hori, T. Behnke, C.A. Motoshima, H. Fox, B.A. Le Trong, I. Teller, D.C. Okada, T. Stenkamp, R.E. Yamamoto, M. and Miyano, M. (2000) *Science*, **289** (5480) 739–745.

Pervushin, K. Riek, R. Wider, G. and Wuthrich, K. (1997) *Proc. Natl. Acad. Sci. USA*, **94** (23) 12366–12371.

Peterson, G.L. (1977) *Anal. Biochem.*, **83**, 346–356.

Phillips, W.J. and Cerione, R.A. (1988) *J. Biol. Chem.*, **263** (30) 15498–15505.

Porath, J. Carlsson, J. Olsson, I. and Belfrage, G. (1975) *Nature*, **258** (5536) 598–599.

Reichert, J. and Hofmann, K.P. (1984) *FEBS Lett.*, **168** (1) 121–124.

Ridge, K.D. Abdulaev, N.G. Sousa, M. and Palczewski, K. (2003) *TIBS*, **28** (9) 479–487.

Ruan, B. Fisher, K.E. Alexander, P.A. Doroshko, V. and Bryan, P.N. (2004) *Biochemistry*, **43** (46) 14539–14546.

Schmitt, J. Hess, H. and Stunnenberg, H.G. (1993) *Mol. Biol. Rep.*, **18** (3) 223–230.

Skiba, N.P. Bae, H. and Hamm, H.E. (1996) *J. Biol. Chem.*, **271** (1) 413–424.

Slep, K.C. Kercher, M.A. He, W. Cowan, C.W. Wensel, T.G. and Sigler, P.B. (2001) *Nature*, **409** (6823) 1071–1077.

Sondek, J. Lambright, D.G. Noel, J.P. Hamm, H.E. and Sigler, P.B. (1994) *Nature*, **372** (6503) 276–279.

Sunahara, R.K. Tesmer, J.J.G. Gilman, A.G. and Sprang, S.R. (1997) *Science*, **278** (5345) 1943–1947.

Teller, D.C. Okada, T. Behnke, C.A. Palczewski, K. and Stenkamp, R.E. (2001) *Biochemistry*, **40** (26) 7761–7772.

Wall, M.A. Coleman, D.E. Lee, E. Iniguezlluhi, J.A. Posner, B.A. Gilman, A.G. and Sprang, S.R. (1995) *Cell*, **83** (6) 1047–1058.